Velocity-matched slow-wave electrodes for integrated electro-optic modulators

Nicolas A. F. Jaeger and Zachary K. F. Lee

University of British Columbia, Department of Electrical Engineering
Vancouver, British Columbia, Canada V6T 1Z4

ABSTRACT

Coplanar slow-wave electrode structures capable of matching the velocities of microwaves to those of optical waves in compound semiconductor based electro-optic modulators are described. In such an electrode microwaves are slowed by periodically adding pairs of capacitive loading fins to the electrode to increase its capacitance per unit length, without obtaining a corresponding decrease in its inductance per unit length. Electro-optic modulators having wide bandwidths and requiring small amounts of modulating power may be realized by using slow-wave electrodes to achieve the velocity-match condition. The theory of operation of, and the results of some measurements on, electrodes of this type are presented.

1. INTRODUCTION

The velocity mismatch between an optical signal and a microwave signal in a conventional integrated electro-optic travelling-wave modulator is a fundamental problem[1,2]. When a velocity mismatch exists there is a change in phase of the modulating signal, the microwave, as "seen" by the modulated signal, the optical wave, as the two propagate down the modulator. To reduce this effect the interaction lengths between the microwave and the optical wave are kept relatively short; however, the use of short interaction lengths increases the power needed to obtain a given modulation. In other words, there is a limit on the bandwidth that may be achieved per unit modulating power. On the other hand, if the microwave and optical wave velocities are matched, then the interaction lengths can be made very long, limited only by attenuation. Since the voltage-length product characterizes electro-optic modulators of this type[1,2], when the length need not be limited, the power needed to achieve a given modulation may be made arbitrarily small. In this paper a slow-wave electrode structure, that can be easily fabricated on gallium arsenide and indium phosphide based materials and that can be used to obtain the needed velocity-match[3,4,5] condition, is described.

Here we are concerned with electro-optic modulators fabricated using compound semiconductors since in conventional lithium niobate based modulators the optical wave travels faster than the microwave. In other words, in lithium niobate based modulators a fast-wave electrode would be needed to achieve velocity-match, whereas in modulators fabricated using gallium arsenide or indium phosphide based materials the microwave travels faster than the optical wave and a slow-wave electrode may be used[3,4,5]. In this paper we give the theory of operation of our slow-wave electrodes, investigate their high frequency potential, and present the results of some measurements on such structures.

0-8194-0999-5/93/$4.00

2. THEORY

The microwave is slowed as a result of the increased capacitance per unit length, without a corresponding decrease in the inductance per unit length, of these electrodes, brought about by the periodic addition of narrow capacitive loading fins[3,4,5]. Capacitive loading fins of length l and width W_2 are added in opposing pairs, separated by a gap of width S_2 and having a period d, to coplanar strips of width W_1 separated by a gap of width S_1; both the fins and the coplanar strips are of thickness t. The structure is shown in Figure 1. The fins must be narrow to effectively load the strips, since narrow fins have a higher capacitance to fin length ratio than wide fins and since narrow fins can increase the capacitance per unit length while having comparatively little effect on the inductance per unit length; here, the word "narrow" means having a large W_2 to l ratio.

To determine the high frequency potential of our slow-wave electrodes we have modelled them as lossless and have treated the fins as being purely capacitive, see Figure 2. The slow-wave electrode is divided into sections and a transfer matrix method is used[6,7,8]. Across any particular section the voltage and current on one side are related to the voltage and current on the other side by a 2 × 2 matrix. In the model shown, the slow-wave (loaded) electrode consists of two sections of unloaded electrode, each extending a distance $d/2$ in either direction from the centre of an opposing pair of fins, and a central capacitive section, consisting of the opposing pair of fins. Using network analysis, the voltage V and current I for the nth and $(n+1)^{th}$ sections are related by

$$\begin{bmatrix} V_n \\ I_n \end{bmatrix} = \begin{bmatrix} \cos\frac{kd}{2} & jZ_o\sin\frac{kd}{2} \\ \frac{j}{Z_o}\sin\frac{kd}{2} & \cos\frac{kd}{2} \end{bmatrix} \begin{bmatrix} 1 & 0 \\ j\omega C_f & 1 \end{bmatrix} \begin{bmatrix} \cos\frac{kd}{2} & jZ_o\sin\frac{kd}{2} \\ \frac{j}{Z_o}\sin\frac{kd}{2} & \cos\frac{kd}{2} \end{bmatrix} \begin{bmatrix} V_{n+1} \\ I_{n+1} \end{bmatrix}$$

$$= \begin{bmatrix} \cos kd - \frac{\omega C_f Z_o}{2}\sin kd & j\left(Z_o\sin kd + \frac{Z_o^2\omega C_f}{2}\cos kd - \frac{Z_o^2\omega C_f}{2}\right) \\ j\left(\frac{1}{Z_o}\sin kd + \frac{\omega C_f}{2}\cos kd + \frac{\omega C_f}{2}\right) & \cos kd - \frac{\omega C_f Z_o}{2}\sin kd \end{bmatrix} \begin{bmatrix} V_{n+1} \\ I_{n+1} \end{bmatrix} \tag{1}$$

where C_f, ω, Z_o, and k are, respectively, the capacitance of a pair of fins, the radian frequency of the microwave, the characteristic impedance of an unloaded electrode, and the propagation constant for an unloaded electrode. Equation (1) can be written in terms of an equivalent transfer matrix

$$\begin{bmatrix} V_n \\ I_n \end{bmatrix} = \begin{bmatrix} \cos\beta d & jZ'\sin\beta d \\ \frac{j}{Z'}\sin\beta d & \cos\beta d \end{bmatrix} \begin{bmatrix} V_{n+1} \\ I_{n+1} \end{bmatrix} \tag{2}$$

where β and Z' are the propagation constant and the characteristic impedance of the loaded electrode, respectively. β is given by

$$\beta = \frac{N_{eff}}{N_o} k \tag{3}$$

where N_{eff} and N_o are, respectively, the effective refractive indices for the loaded and the unloaded electrodes, and, in turn, N_o is given by

$$N_o = \sqrt{\frac{\epsilon_r + 1}{2}} \tag{4}$$

where ϵ_r is the relative permittivity of the substrate (here the superstrate is assumed to be air having a relative permittivity of 1). From equations (1) and (2) one obtains

$$\cos\beta d = \cos kd - \frac{\omega C_f Z_o}{2} \sin kd \tag{5}$$

and

$$Z' = Z_o \left[1 - \frac{\omega C_f}{\frac{1}{Z_o} \sin kd + \frac{\omega C_f}{2} \cos kd + \frac{\omega C_f}{2}} \right]^{1/2} \tag{6}$$

Equations (3), (5) and (6) provide useful information on the characteristics of the slow-wave electrodes: N_{eff}, dispersion, phase velocity, group velocity, and high frequency filter characteristics.

The slow-wave electrode's phase and group velocities ($v_p = \omega/\beta$ and $v_g = d\omega/d\beta$) are found by solving Equation (5). Figure 3 shows v_p and v_g vs. frequency for a typical structure on gallium arsenide ($\epsilon_r = 12.9$ [9]) that meets the velocity-match condition $N_{eff} = 3.43$; for this case we set $l = 1$ μm, $W_2 = 7$ μm, $S_2 = 1$ μm, and $t = 0.5$ μm, and calculated $d = 7.3$ μm and $Z_o = 65$ ohm. Figure 4 shows ω vs. β; it is apparent that at very high frequencies, when the fin spacing d becomes comparable to a wavelength, the electrode begins to behave like a band-pass filter. The transmission of the slow-wave electrode will be cut off when the lowest stop-band is reached. Figure 5 shows Z' vs. frequency.

In the foreseeable future modulators using these electrode structures would probably operate at frequencies that are far lower than the lowest stop-band frequency. In this regime the fin spacing is much smaller than the wavelength of the microwave so that $\beta d \ll 1$ and $kd \ll 1$. Therefore, equations (5) and (6) can be simplified. Using $N_o = c[LC]^{1/2}$ and $Z_o = [L/C]^{1/2}$ [6] it can be shown that the effect of adding the fins simply amounts to increasing C to $C + C_f/d$, where c, L, and C are, respectively, the speed of light in vacuum, the inductance per unit length, and the capacitance per unit length[5]. Up to this point we have assumed that the fins were purely capacitive elements and that they did not change the inductance per unit length. To allow for changes in the inductance per unit length a weighted average was used[3,5] such that N_{eff} and Z' are given by

$$N_{eff} = \sqrt{\left[Z_o(1-\frac{l}{d}) + Z_1\frac{l}{d}\right]\left[\frac{N_o^2}{Z_o} + \frac{C_f C}{d}N_o\right]} \tag{7}$$

and

$$Z' = \sqrt{\left[Z_o(1-\frac{l}{d}) + Z_1\frac{l}{d}\right]\left[\frac{N_o}{\frac{N_o}{Z_o} + \frac{C_f C}{d}}\right]} \tag{8}$$

where Z_1 is the characteristic impedance of an unloaded electrode with a gap width of S_2 and having strips of width $W_1 + W_2$. From equations (7) and (8) the design formulas[3,5] can be obtained:

$$N_{eff}Z' = \left[Z_o(1-\frac{l}{d}) + Z_1\frac{l}{d}\right]N_c \tag{9}$$

and

$$\frac{N_{eff}}{Z'} = \frac{N_o}{Z_o} + \frac{C_f C}{d}. \tag{10}$$

For the structures considered Z_1 is typically significantly less than Z_o and, hence, the term $Z_1 l/d$ may be ignored. The capacitance between two fins was calculated for various fin dimensions using both finite difference[10,11,12] and finite element[13] methods. Design curves for 50 ohm electrodes on gallium arsenide ($\epsilon_r = 12.9$, $N_{eff} = 3.43$ [1,2]) and indium phosphide ($\epsilon_r = 12.4$, $N_{eff} = 3.24$ [14,15]) substrates were generated; these are given in Figures 6 and 7, respectively. Here, the electrodes were assumed to be half-buried in the substrate; however, the curves can still be used for surface deposited electrodes when they are relatively thin. In designing the electrodes, one first chooses the dimensions of the fins to be used, then d and Z_o are obtained from these curves. The value of W_1 is simply that for a pair of unloaded coplanar strips having the Z_o given by the curves[16,17].

3. MEASUREMENTS

In order to verify our theory half-buried aluminum slow-wave electrodes were fabricated on gallium arsenide substrates and their N_{eff}'s were measured. They were fabricated using a single-step lift-off technique[9]. The electrodes were half-buried in the substrate by performing a controlled etch prior to depositing the aluminum.

To measure the N_{eff}'s we used a resonance technique. The equipment used included a microwave scalar network analyzer, a synthesized microwave signal source, and a coplanar strip probe. The network analyzer was calibrated at the probe tip and was set up to measure the normalized reflected power, i.e., 10log(reflected power/incident power), as a function of frequency. Due to the slight mismatch between the probe and the electrode, some of the

microwave was reflected back into the electrode, producing resonance. The N_{eff}'s were calculated by measuring the frequency separation between the peaks of the resonances using

$$N_{eff} = \frac{c}{2L_{el}} \frac{1}{\Delta f} \tag{11}$$

where L_{el} is the length of the electrode and Δf is the frequency separation between two adjacent peaks. Figures 8 and 9 give the normalized reflected power vs. frequency for two electrodes. These electrodes had dimensions ~ 4× those that would probably be used in an electro-optic modulator, which allowed us to use photo-generated, as opposed to electron-beam generated, masks in their fabrication.

The dimensions, theoretically predicted N_{eff}'s and ΔN_{eff}'s, measured N_{eff}'s and ΔN_{eff}'s, for these electrodes are given in Table 1; ΔN_{eff} is the difference between the effective refractive index of a particular slow-wave electrode and that of an unloaded electrode. The accuracy of the measurements for the N_{eff}'s was ~ ± 0.05. As a comparison, both the theoretically predicted and measured N_{eff}'s of an unloaded electrode are given. The measurement results and the theoretically predicted values show good agreement, especially for ΔN_{eff}.

4. SUMMARY

In this paper we have presented the results of calculations of the high frequency characteristics of our slow-wave electrode structures using a transfer matrix method. The calculations indicate that the filter characteristics of such an electrode having typical dimensions will only become apparent at frequencies in the THz range. In the foreseeable future, modulators using such electrode structures would probably be used at much lower frequencies. Design formulas for these slow-wave electrodes are reviewed and design curves are provided for electrodes fabricated on gallium arsenide and indium phosphide substrates, with air as the superstrate. Finally, the results of the measurements of the N_{eff}'s of two such electrode structures are presented, showing good agreement between the measurements and the theoretically predicted values.

5. ACKNOWLEDGEMENTS

The authors gratefully acknowledge the support of the Canadian Cable Labs Fund and the Natural Sciences and Engineering Research Council (NSERC) of Canada for their generous financial support of this work.

6. REFERENCES

1. R. C. Alferness, "Waveguide Electrooptic Modulators," *IEEE Trans. Microwave Theory Tech.*, vol. MTT-30, no. 8, pp. 1121-1137, 1982.
2. R. C. Alferness, "Titanium-Diffused Lithium Niobate Waveguide Devices," in Guided-Wave Optoelectronics, T. Tamir, Ed., pp. 145-210, Springer Series in Electronics and Photonics 26, Springer-Verlag Berlin Heidelberg, 1988.

3. N. A. F. Jaeger and Z. K. F. Lee, "Slow-Wave Electrode for Use in Compound Semiconductor Electro-Optic Modulators," *IEEE J. Quantum Electron.*, vol. QE-28, no. 8, pp. 1778-1784, 1992.
4. Z. K. F. Lee and N. A. F. Jaeger, "Electrode Structures for Microwave to Optical Wave Velocity-Match in III-V Semiconductor Electro-Optic Modulators," *IEEE CLEO Conf. Technical Digest*, paper no. CThS5, Anaheim, CA., U. S. A., May 10-15, 1992.
5. Z. K. F. Lee, "Slow-Wave Electrode Structures for III-V Semiconductor Based Electro-Optic Travelling-Wave Modulators," M. A. Sc. Thesis, The University of British Columbia, April, 1992.
6. R. E. Collin, Foundations for Microwave Engineering, pp. 363-381, McGraw-Hill, New York, 1966.
7. A. F. Harvey, "Periodic and Guiding Structures at Microwave Frequencies," *IRE Trans.*, vol. MTT-8, pp. 30-61, 1960.
8. A. W. Lines, G. R. Nicoll, and A. M. Woodward, "Some Properties of Waveguides with Periodic Structure," *Proc. IEE*, vol. 97, pt. III, pp. 263-276, 1950.
9. R. Williams, Modern GaAs Processing Methods, pp. 25-26, 96-106, 115-138, Artech House, Massachusetts, 1990.
10. D. H. Sinnott, G. K. Cambrell, C. T. Carson, and H. E. Green, "The Finite Difference Solution of Microwave Circuit Problems," *IEEE Trans. Microwave Theory Tech.*, vol. MTT-17, no. 8, pp. 464-478, 1969.
11. D. H. Sinnott, "The Use of Interpolation in Improving Finite Difference Solutions of TEM Mode Structures," *IEEE Trans. Microwave Theory Tech.*, vol. MTT-17, no. 1, pp. 20-28, 1969.
12. J. W. Duncan, "The Accuracy of Finite Difference Solutions of Laplace's Equation," *IEEE Trans. Microwave Theory Tech.*, vol. MTT-15, no. 10, pp. 575-582, 1967.
13. A. E. Ruehli and P. A. Brennan, "Efficient Capacitance Calculations for Three-Dimensional Multiconductor Systems," *IEEE Trans. Microwave Theory Tech.*, vol. MTT-21, no. 2, pp. 76-82, 1973.
14. M. S. Whalen and J. Stone, "Index of Refraction of n-type InP at 0.663 μm and 1.15 μm Wavelengths as a Function of Carrier Concentration," *J. Appl. Phys.*, vol. 53, no. 6, pp. 4340-4343, 1982.
15. J. P. Donnelly, N. L. DeMeo, F. J. Leonberger, S. H. Groves, P. Vohl, and F. J. O'Donnell, "Single-Mode Optical Waveguides and Phase Modulators in the InP Material System," *IEEE J. Quantum Electron.*, vol. QE-21, no. 8, pp. 1147-1151, 1985.
16. K. C. Gupta, R. Garg, and I. J. Bahl, Microstrip Lines and Slotlines, pp. 257-288, Artech House, Massachusettes, 1979.
17. C. P. Wen, "Coplanar Waveguide: A Surface Strip Transmission Line Suitable for Nonreciprocal Gyromagnetic Device Applications," *IEEE Trans. Microwave Theory Tech.*, vol. MTT-17, no. 12, pp. 1087-1091, 1969.

Table 1. Dimensions, N_{eff}'s, and ΔN_{eff}'s of two slow-wave electrodes.

S_1 = 60 μm, S_2 = 4 μm, W_2 = 28 μm, l = 4 μm, t = 1.1 μm						
Electrode	W_1	d	N_{eff} (predicted)	ΔN_{eff} (predicted)	N_{eff} (measured)	ΔN_{eff} (measured)
#1	72	18	3.50	0.86	3.40	0.80
#2	110	32	3.16	0.52	3.10	0.50
unloaded electrode			2.64	--	2.60	--

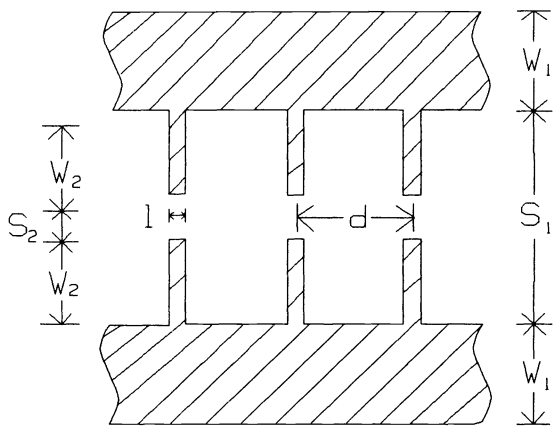

Figure 1. A plan view of a section of a slow-wave electrode showing the dimensions S_1, W_1, S_2, W_2, d, and l.

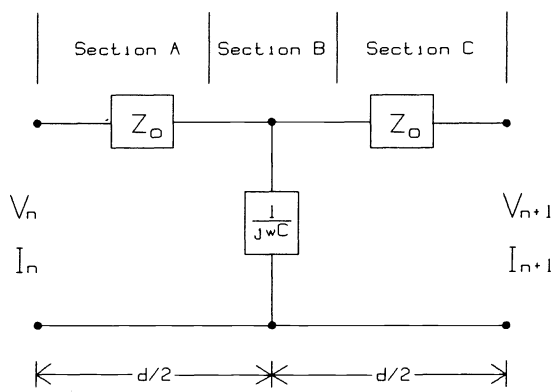

Figure 2. The model used for our transfer matrix analysis.

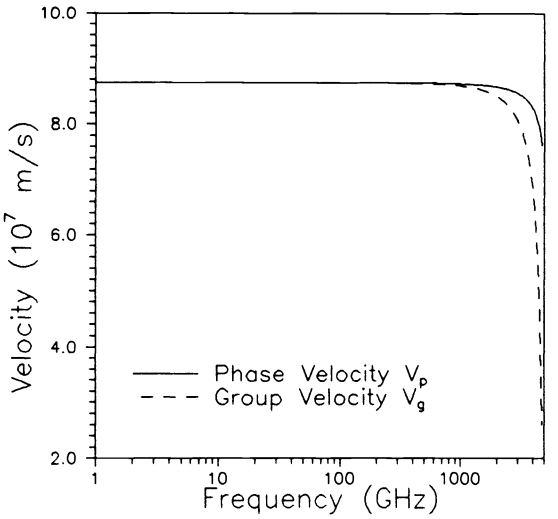

Figure 3. The phase and group velocities vs. frequency for a typical slow-wave electrode.

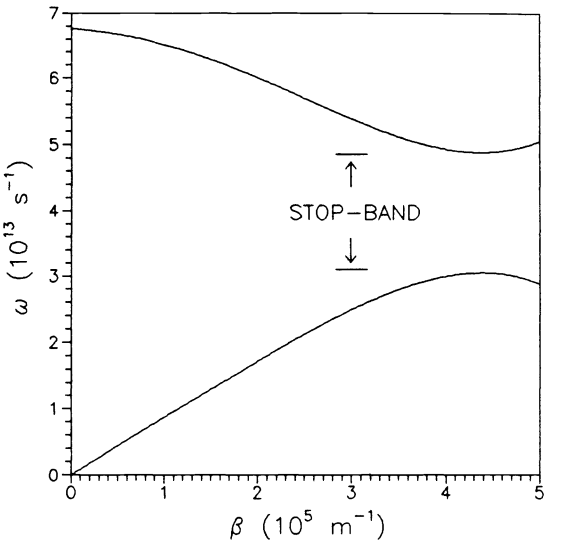

Figure 4. ω vs. β curves for the lowest two pass-bands of a typical slow-wave electrode.

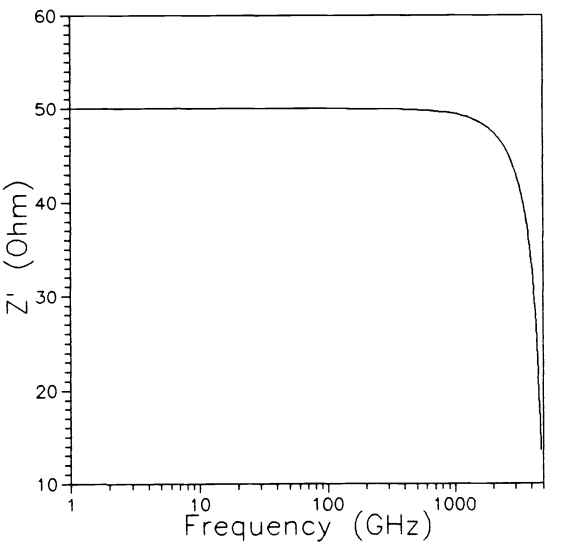

Figure 5. Characteristic impedance vs. frequency for a typical lossless slow-wave electrode.

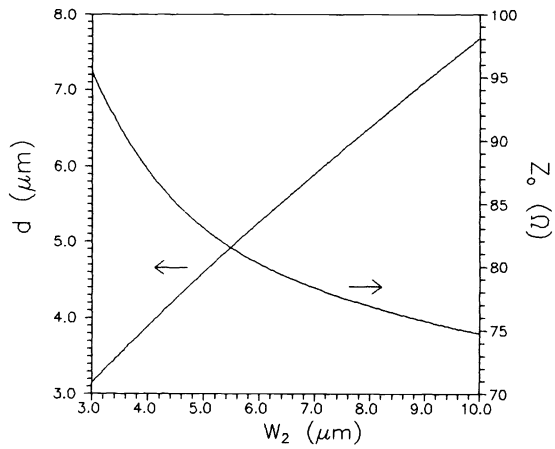

Figure 6. Design curves for 50 ohm velocity-matched slow-wave electrodes on GaAs substrates for $S_2 = 1\ \mu m$, $l = 1\ \mu m$, and $t = 0.5\ \mu m$.

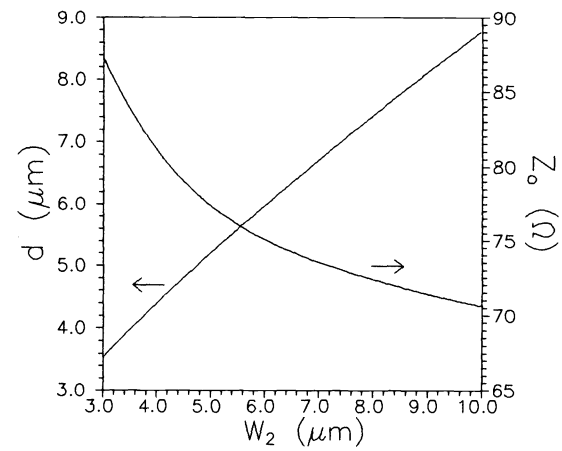

Figure 7. Design curves for 50 ohm velocity-matched slow-wave electrodes on InP substrates for $S_2 = 1\ \mu m$, $l = 1\ \mu m$, and $t = 0.5\ \mu m$.

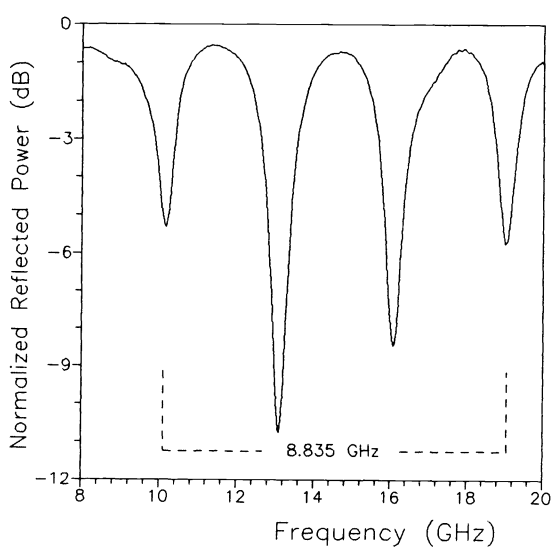

Figure 8. Measured normalized reflected power vs. frequency for electrode #1 of Table 1.

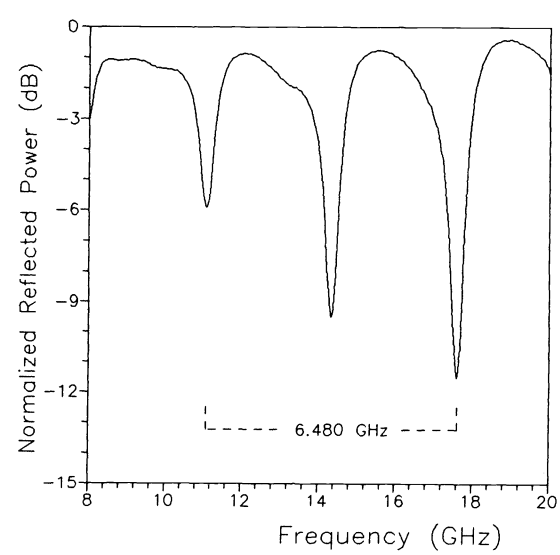

Figure 9. Measured normalized reflected power vs. frequency for electrode #2 of Table 1.